Cell Cycle 14:9, 1459–1470; May 1, 2015; Published with license by Taylor & Francis

Stranglehold on the spindle assembly checkpoint: the human papillomavirus E2 protein provokes BUBR1-dependent aneuploidy

Chye Ling Tan[1,2,#], Sébastien Teissier[1,#], Jayantha Gunaratne[3], Ling Shih Quek[1], and Sophie Bellanger[1,*]

[1]Cell Cycle Control in Skin Epidermis; Institute of Medical Biology; A*Star, Biopolis; Immunos, Singapore; [2]Current address: Department of Pathology; Singapore General Hospital; The Academia, Singapore; [3]Quantitative Proteomic Group; Institute of Molecular and Cell Biology; A*Star; Biopolis; Proteos, Singapore

[#]These authors contributed equally to this work.

Keywords: aneuploidy; BUBR1; E2; mitosis; papillomavirus; p53; spindle assembly checkpoint

Abbreviation list: HPV, Human Papillomavirus; SAC, Spindle Assembly Checkpoint; MCC, Mitotic Checkpoint Complex; APC/C, Anaphase Promoting Complex/Cyclosome; E2 TAD, E2 Transactivation Domain; E2 ΔTAD, E2 deleted of the Transactivation Domain; Ad, Adenovirus; Thym, Thymidine; Noco, Nocodazole; GFP, Green Fluorescent Protein; MS, Mass Spectrometry; m.o.i., Multiplicity of Infection.

The Human Papillomavirus (HPV) E2 protein, which inhibits the E6 and E7 viral oncogenes, is believed to have anti-oncogenic properties. Here, we challenge this view and show that HPV-18 E2 over-activates the Spindle Assembly Checkpoint (SAC) and induces DNA breaks in mitosis followed by aneuploidy. This phenotype is associated with interaction of E2 with the Mitotic Checkpoint Complex (MCC) proteins Cdc20, MAD2 and BUBR1. While BUBR1 silencing rescues the mitotic phenotype induced by E2, p53 silencing or presence of E6/E7 (inactivating p53 and increasing BUBR1 levels respectively) both amplify it. This work pinpoints E2 as a key protein in the initiation of HPV-induced cervical cancer and identifies the SAC as a target for oncogenic pathogens. Moreover, our results suggest a role of p53 in regulating the mitotic process itself and highlight SAC over-activation in a p53-negative context as a highly pathogenic event.

Introduction

HPV (Human Papillomavirus) infection was first linked to cervical cancer in 1976,[1] and is now accepted as the main causative agent of this disease. It specifically infects the basal epithelial cells of the skin, oral and ano-genital tract. Around 120 different HPV genotypes have been described, with a range of oncogenic potentials. While low-risk HPV genotypes (such as HPV-6 and 11) never induce cancer, the high-risk HPV-16 and 18 types together account for 70% of cervical carcinoma cases.[2] Strikingly, despite the first release of 2 vaccines against HPV in 2006–2007, 8 years later cervical cancer continues to claim more than a quarter of a million lives each year worldwide, with 500000 new cases diagnosed. These statistics highlight a need for development of new therapeutics against cervical carcinoma as well as for discovery of drugs able to prevent transformation of benign HPV lesions.

The HPV genome comprises 6 early genes (E1, E2, E4, E5, E6 and E7), 2 late genes (L1 and L2) and a non-coding control region. The E6 and E7 proteins, which inhibit p53 and pRB respectively,[3-7] are the 2 best characterized HPV oncogenes. In contrast, the E2 protein represses their transcription and is therefore classified as a viral anti-oncogene.[8,9] In benign HPV lesions, the HPV DNA keeps its episomic (circular) structure, therefore allowing expression of the full HPV genome. In contrast, during carcinogenesis the viral DNA usually integrates into the cellular genome, leading to loss of parts of HPV DNA. Similar to cellular anti-oncogenes which are frequently inactivated in cancer, expression of E2 is often lost following this integration.[10-12] The mechanism of integration remains unknown, but because the resulting loss of E2 allows E6/E7 expression, integration is considered as a key event in transformation by HPV.

Despite the obvious anti-proliferative activities of high-risk HPV E2, there were hints of another side of E2, at least in HPV-independent systems. Indeed, it has been shown that transgenic mice expressing E2 from the high-risk HPV-8 in the skin epithelium develop hyperplasia and skin tumors,[13,14] while under similar conditions the low-risk HPV-11 E2 protein has no effect.[15] Three years before these publications, we had published that in

*Correspondence to: Sophie Bellanger; Email: sophie.bellanger@imb.a-star.edu.sg
Submitted: 11/13/2014; Revised: 01/28/2015; Accepted: 02/14/2015
http://dx.doi.org/10.1080/15384101.2015.1021519

HPV-negative cells, E2 from HPV-18 and 16, but not from HPV-6 and 11, induced chromosomal instability during anaphase coupled to metaphase delay and lack of degradation of APC^{Cdc20} (Anaphase Promoting Complex) substrates like cyclin B.[16] This property is mediated by the N-terminal Transactivation Domain of E2 (TAD, amino-acids 1–206) which binds Cdc20 and which is sufficient to mediate similar effects on mitosis as full-length E2. In contrast, an E2 protein deleted of this TAD domain (ΔTAD) loses binding to Cdc20, no longer induces mitotic abnormalities and does not stabilize cyclin B.[16] Since APC^{Cdc20} is the mitotic ubiquitin-ligase that triggers the metaphase-to-anaphase transition by targeting cell cycle proteins (including cyclin B) for degradation, we postulated in this article that interaction of the TAD domain of E2 with Cdc20 inhibited APC^{Cdc20} activity, explaining the mitotic phenotypes observed.[16] Nevertheless, the mechanism of inhibition of APC^{Cdc20} by HPV E2 has not been elucidated.

APC^{Cdc20} activity is carefully monitored by the Spindle Assembly Checkpoint (SAC). The SAC mediates the formation of the MCC (Mitotic Checkpoint Complex), whose main components BUBR1 and MAD2 target Cdc20 to inhibit APC^{Cdc20} activity.[17] This mechanism allows inhibition of mitotic exit until completion of chromosome alignment on the metaphasic plate. Once this condition is achieved, the MCC disassembles, allowing activation of APC^{Cdc20} and anaphase onset.

Here, we show that not only does HPV-18 E2 interact with Cdc20, but it also binds to the MCC proteins MAD2 and BUBR1. Using RNA-interference, we identified the presence of BUBR1 as essential for the abnormal mitotic phenotype induced by E2, which interestingly is amplified by loss of p53. These data highlight gaps in our knowledge of HPV-driven carcinogenesis. They call into question the current perception of E2 as a purely anti-oncogenic protein and pinpoint over-activation of the SAC in a p53-negative context as mutagenic.

Results

E2 arrests the cell cycle in mitosis and induces aneuploidy in the C33-A keratinocyte cell line

HPV-18 and 16 E2 proteins arrest the cell cycle in mitosis and lead to mitosis-induced chromosomal instability in primary fibroblasts and in Saos-2 cells (p53-null osteocarcinoma cell line).[16] To get further insights into the mechanism by which high-risk HPV E2 induces mitotic defects, we decided to establish the HPV-18 E2 interactome using mass spectrometry (MS). We selected the C33-A cell line, derived from a HPV-negative human cervical carcinoma biopsy, and first verified that E2 could also induce a mitotic arrest in these cells. HPV-18 E2 (and deletants of E2) were fused to GFP and expressed using adenoviral infections. Importantly, in this article we used multiplicities of infection (m.o.i.) between 20 and 200 depending on experiments (200 in this specific experiment). We have previously shown that E2 expression levels in HPV lesions (CIN-I) are in fact higher than those obtained after infection of keratinocytes at m.o.i. 200 with the adenovirus expressing GFP-E2.[18,19] Therefore, all m.o.i. used in this article give E2 expression levels within the range of E2 physiological levels. Cells were infected by recombinant adenoviruses (Ad) expressing GFP fused to the full-length HPV-18 E2 protein (GFP-E2), GFP fused to the E2 protein deleted of its transactivation domain (GFP-ΔTAD), or GFP alone (GFP). Structures of the fusion proteins are shown in **Figure 1A**. DNA content was analyzed by flow cytometry 36 hours after infection. In an asynchronous population expressing GFP-E2, 6–7% more of the cells were in G2/M compared to a population expressing GFP or GFP-ΔTAD (**Fig. 1A**). To amplify the phenotype and more accurately quantify it, infected cells were synchronized at the G1/S transition using thymidine, before being released into the cell cycle. Cells were labeled for Ser10-phosphorylated histone H3 (which specifically identifies mitotic cells) to differentiate between G2 and M. Fourteen hours after thymidine release, control cells have exited mitosis and entered the next G1 phase (**Fig. 1B**, GFP Thym R14). In contrast, GFP-E2-expressing cells experienced a strong mitotic arrest characterized by a 39% G2/M peak in which more than half of the cells were in mitosis (**Fig. 1B**). As expected from our previous publication,[16] GFP-ΔTAD-expressing cells showed a normal phenotype similar to GFP.

Interestingly, a substantial proportion of asynchronous C33-A cells expressing E2 (18.4%) appears aneuploid with a >4N DNA content (**Fig. 1A**). Since we have shown that abnormal segregation of chromosomes occurs during anaphase in E2-expressing cells,[16] supernumerary DNA acquired during mitosis could lead to the appearance of this aneuploid population after the next S-phase. Alternatively, these cells might result from endo-replication cycles during S-phase. However, the synchronization experiment shown in **Figure 1B** allowed us to distinguish between these 2 scenarios. If E2 induced endo-replication, the percentage of aneuploid cells should be much higher in synchronized cells (which are all going through S simultaneously) than in an asynchronous population. Since only 9.8% of E2-expressing cells were aneuploid in the released synchronized population (compared to 18.4% for asynchronous cells), we concluded that aneuploidy was most likely a consequence of chromosomal abnormalities acquired during mitosis rather than endo-replication.

By performing Comet assays in similar conditions of synchronization, we could visualize induction of DNA breaks by E2 following mitosis in early G1 (Thym R14), which probably account for the appearance of the aneuploid population. As shown in **Figure 1C**, tails appeared in about 5–10% of GFP-E2-expressing cells whereas they were absent in GFP- and GFP-ΔTAD-expressing cells. In conclusion, in C33-A cells, full-length E2 induces a mitotic arrest, DNA breaks during mitosis and aneuploidy.

E2 interacts with the mitotic checkpoint complex and regulators of mitotic completion

In order to identify the cellular interaction partners of E2 involved in the mitotic arrest observed in C33-A cells, lysates of GFP-E2- or GFP-infected cells were subjected to immunoprecipitation followed by Liquid Chromatography-Mass Spectrometry/Mass Spectrometry (LC-MS/MS) experiments (**Fig. S1A-B** and Supplementary Materials and Methods for details of MS protocol). Three independent experiments were conducted. The first 2

experiments (MS/MS #1 and MS/MS #2) were replicates performed using classic LC-MS/MS. The 3rd MS was a SILAC experiment (Stable Isotope Labeling by Amino-acids in Cell culture), a quantitative LC-MS/MS-based approach used here to verify and quantify the interactions characterized in the first 2 MS. Analysis of the intersection between the 2 replicates gave us 406 E2 interactants which were further clustered using GeneGo (**Fig. S1C-D**). The protein folder named "Cell cycle and its regulation" was the most significant protein cluster identified in this analysis (**Fig. S1C**). This folder consists of sub-folders from which the "Spindle assembly and chromosome separation" pathway ranked first, and the "Metaphase checkpoint" (=SAC) appeared in fourth position (**Fig. S1D**).

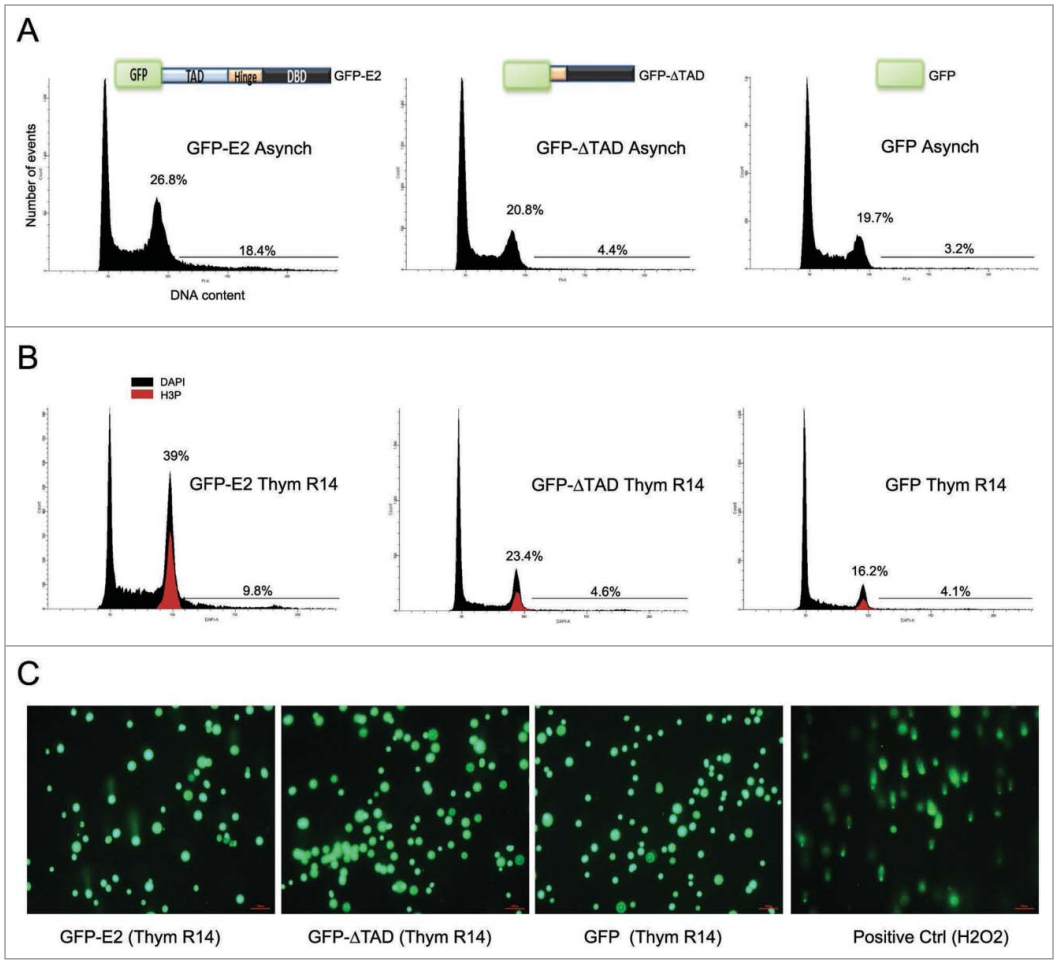

Figure 1. E2 arrests the cell cycle in mitosis and induces DNA breaks and aneuploidy in the C33-A keratinocyte cell line. (**A**) Asynchronous (Asynch) C33-A cells were infected by AdGFP-E2, AdGFP-ΔTAD or AdGFP. The structure of the different proteins are shown (TAD=Transactivation Domain, DBD=DNA Binding Domain). After 36 hours, DNA was stained with propidium iodide for cell cycle analysis by flow cytometry. (**B**) C33-A cells were infected and synchronized at the G1/S transition using thymidine before being released for 14 hours (Thym R14). Mitotic cells labeled by anti-phosphorylated histone H3 (H3P) are shown in red. DNA was stained with DAPI. (**C**) Comet assays performed from cells synchronized by thymidine at the G1/S transition and released for 14 hours. Treatment with H2O2 was used as a positive control.

The SAC component BUBR1 was found in the 2 sub-folders described above, as were proteins of the mitotic spindle like α-, β-, and γ-tubulins, and a number of kinetochore proteins (**Fig. 2A** for simplified table and **Table S1** for detailed results). The MAD2 protein was not found in the initial analysis because it only appeared in one of the first 2 MS. However, it was found with a significant ratio (3.3) in the SILAC experiment and was further confirmed by both immunofluorescence and co-immunoprecipitation/western-blot (see below). Most of the other SAC and mitotic spindle interactants were also confirmed by SILAC (using a cut-off ratio ≥1.4), showing the reliability of the results (**Table S1**).

We then went on to visualize the interactions of the MCC proteins with E2 by immunofluorescence using specific antibodies. We could show that BUBR1 and MAD2 partially co-localized with GFP-E2 in metaphasic cells (**Fig. 2B**). Indeed, some E2 dots co-localized with BUBR1 and MAD2 dots, while some dots only appeared adjacent to BUBR1 and MAD2. Since BUBR1 and MAD2 are known to localize, at least partially, at the kinetochores in metaphasic cells, we extended our labeling to include the kinetochore marker CENP-E. E2 co-localized extensively with CENP-E (**Fig. 2B**), thus confirming interaction of E2 at the kinetochores in metaphase. This corroborates results from a previous study showing localization of HPV E2 from some genotypes close to the centromeric regions.[20] We noted that, on top of the punctuate E2 distribution associated with MAD2, BUBR1 and the kinetochores, E2 also appeared as filaments suggestive of microtubules of the mitotic spindle, which are attached to the kinetochores. Microtubules contain α and β-tubulin (which were both identified as E2 interactants by MS), and anti-β-tubulin labeling indeed revealed a near-complete co-localization with E2 (**Fig. 2B**).

To definitively validate the interactions of E2 with the SAC proteins, co-immunoprecipitations of GFP-E2, GFP-TAD, GFP-ΔTAD or GFP with BUBR1, MAD2, and Cdc20, were performed using mitotic extracts (**Fig. 2C**). As published

A

Spindle Assembly Checkpoint	
Cdc20	cell division cycle 20
MAD2	mitotic spindle assembly checkpoint protein MAD2A
BUBR1	BUB1 budding uninhibited by benzimidazoles 1 homolog beta
Kinetochores and SAC regulation	
BRCA2	breast cancer 2, early onset
NUP153	nucleoporin 153kDa
CRM1	exportin 1
DYNC1H1	cytoplasmic dynein 1, heavy chain 1
SMC1A	structural maintenance of chromosomes 1A
SMC3	structural maintenance of chromosomes 3
DCTN1	dynactin 1, isoform 2
Mitotic Spindle	
TPX2	targeting protein for Xklp2
TUBA1A	tubulin alpha-1A chain isoform 1
TUBA1C	tubulin alpha-1C chain
TUBB6	tubulin beta-6 chain
TUBB4	tubulin beta-4 chain
TUBB3	tubulin beta-3 chain isoform 1
TUBB2B	tubulin beta-2B chain
TUBB4B	tubulin beta-4B chain
TUBG1	tubulin gamma-1 chain
KIF22	kinesin-like protein KIF22 isoform 1
MAP1B	microtubule-associated protein 1B

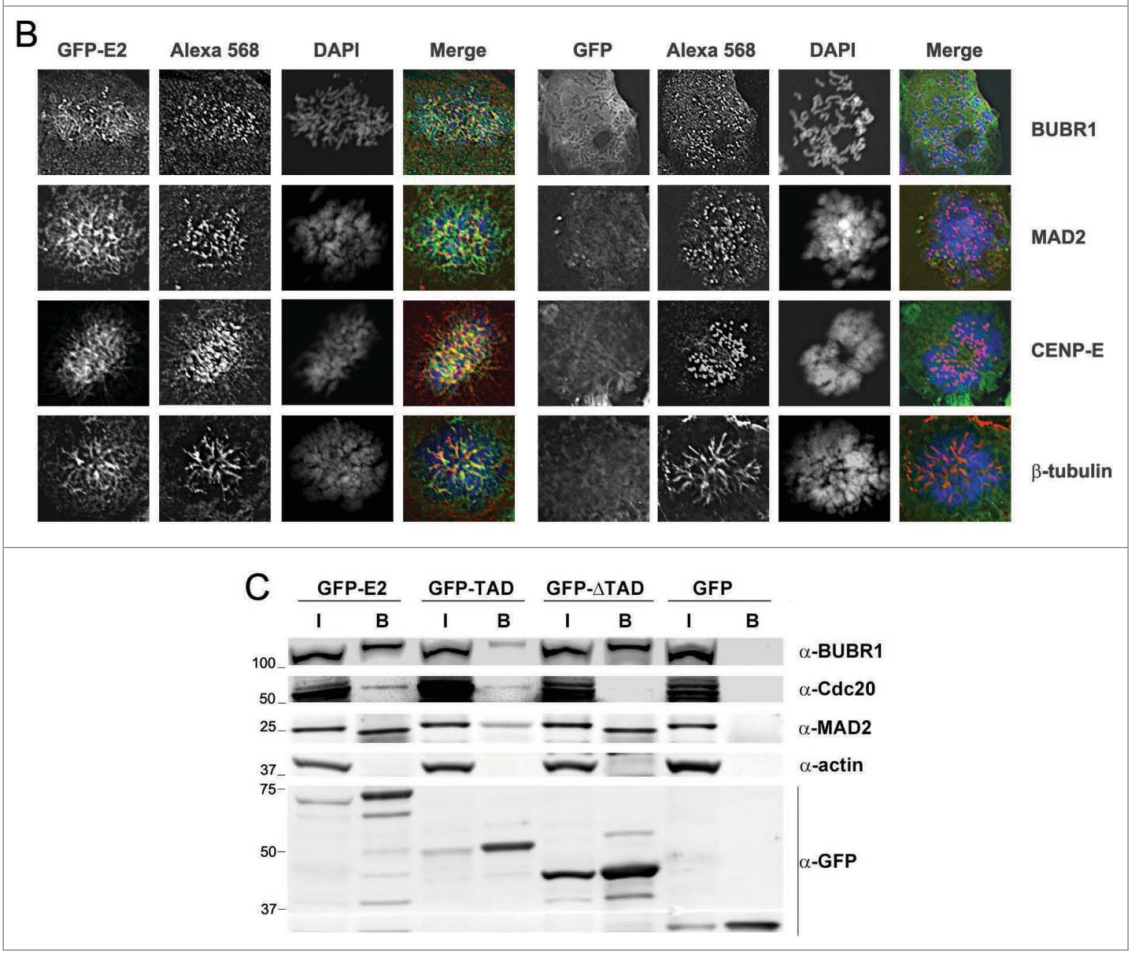

Figure 2. E2 interacts with regulators of mitosis completion including the mitotic checkpoint complex, the spindle itself and the kinetochores. (A) Table listing the interactants of E2 associated with regulation of mitosis completion. See also **Table S1**. (B) Immunofluorescence showing co-localization of GFP-E2 with SAC proteins (BUBR1 and MAD2), kinetochores (CENP-E) and mitotic spindle (β-tubulin). (C) Immunoprecipitation confirming interactions of GFP-E2 with Cdc20, BUBR1 and MAD2 (I = Input, B = Beads).

before,[16,21] we found the E2 interaction with Cdc20 to be mediated by the TAD part only. As expected from our MS and immunofluorescence results, E2 co-immunoprecipitates with both MAD2 and BUBR1. Surprisingly, we detected interactions of BUBR1 and MAD2 with both TAD and ΔTAD. Therefore, it seems that E2 interactions with MAD2 and BUBR1 do not depend on its interaction with Cdc20 (at least for the ΔTAD part). Interestingly, the primarily interaction of TAD with Cdc20 does not depend on MAD2 and BUBR1 either since it has been shown to be direct.[16] However, the interaction of E2 with Cdc20 seems stronger than the one with TAD. It is therefore possible that ΔTAD interactions with MAD2 and BUBR1 stabilize the TAD interaction with Cdc20 by an unknown mechanism. Last but not least, since ΔTAD interacts with MAD2 and BUBR1 but does not induce any abnormal mitoses, this experiment also shows that MAD2 and BUBR1 interactions with the ΔTAD part are not sufficient to mediate the mitotic phenotype in the absence of the TAD-Cdc20 interaction.

E2 prevents SAC inactivation

Since E2 is known to stabilize APC/C substrates like cyclin B,[16] its interaction with the SAC components Cdc20, MAD2, and BUBR1, lead us to suspect that it might inhibit MCC dissociation at the end of metaphase, which would prevent SAC inactivation (rather than activating it directly) and block the cells in mitosis. This prompted us to test the effects of E2 specifically on mitotic exit in HeLa cells. We decided to use this specific cell line because it is a HPV-18-positive cell line, which expresses E6 and E7 but lacks E2 (lost after integration). It is therefore a good system to re-introduce E2 and study its properties in its physiological environment. To specifically look at E2 effects on SAC inactivation, we first had to activate the SAC by an E2-independent stimulus to get rid of E2 effects (if any) on SAC activation at the beginning of mitosis. In order to achieve this, we used nocodazole which is a microtubule drug known to activate the SAC in a reversible manner. We first activated the SAC by nocodazole to block the cells in metaphase. E2 was further expressed in metaphasic cells using adenoviral infection while maintaining the nocodazole treatment for 14 hours. After 14 hours, rounded-up mitotic cells were harvested by mitotic shake-off. A 100% M peak was detected in all populations (**Fig. 3A**, Noco 0). To monitor E2 ability to prevent SAC inactivation, SAC was inactivated by releasing the cells into nocodazole-free medium for 5 hours before flow cytometry analyses

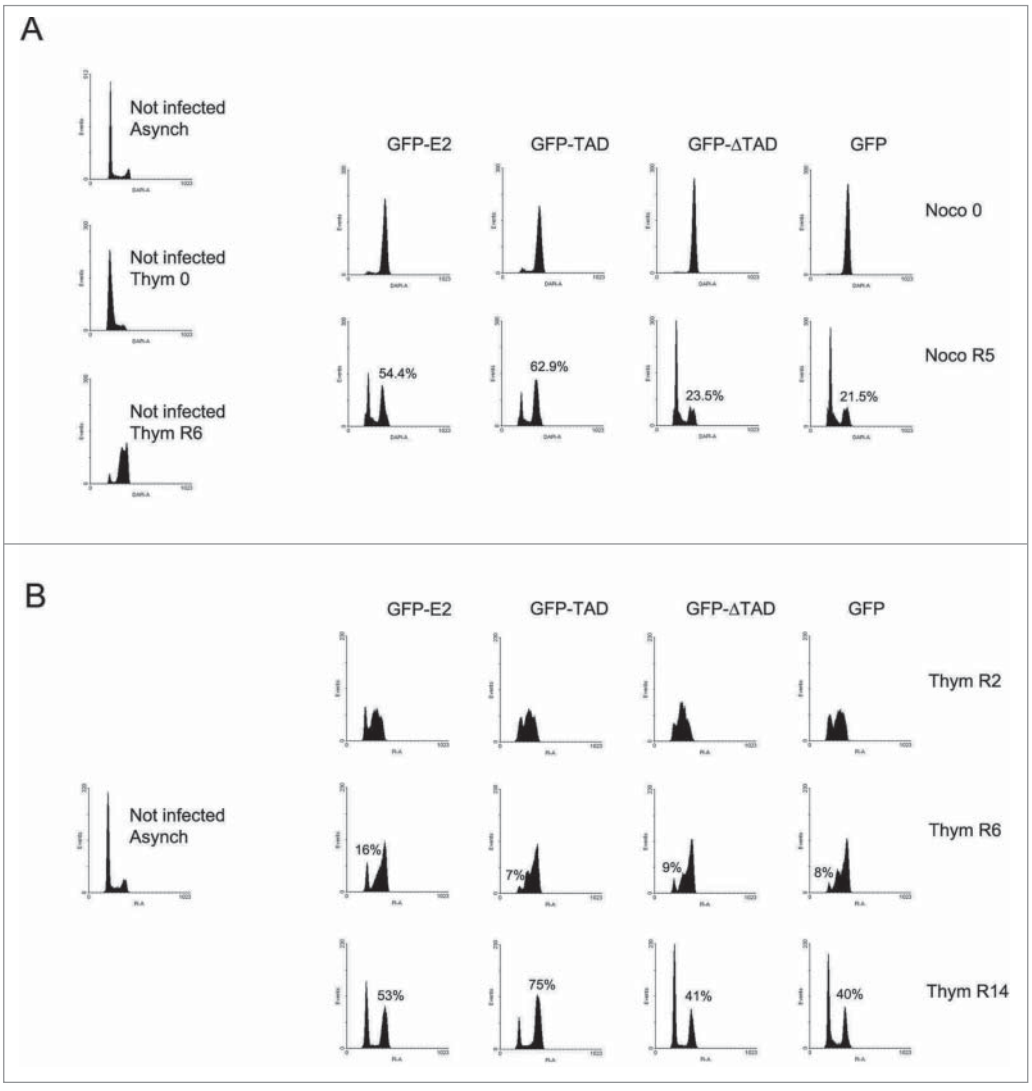

Figure 3. Both E2 and TAD prevent SAC inactivation but TAD is more efficient than E2 in HeLa cells. (**A**) Cell cycle analyses of HeLa cells expressing GFP-E2, GFP-TAD, GFP-ΔTAD or GFP released from nocodazole block. Cells were synchronized in pro-metaphase by successive thymidine/nocodazole treatments. Thym 0 = end of thymidine treatment, Thym R6 = release for 6 hours after thymidine treatment. Six hours after release from thymidine, nocodazole was added to the medium for the next 14 hours. Infection was performed during the nocodazole treatment. After mitotic shake-off (Noco 0), cells were released for 5 hours in nocodazole-free medium (Noco R5). (**B**) Cell cycle analyses of HeLa cells expressing GFP-E2, GFP-TAD, GFP-ΔTAD or GFP, synchronized in the middle of S phase (Thym R2), and released for 4 (Thym R6) or 12 (Thym R14) hours. Infection was performed during the thymidine treatment.

(**Fig. 3A**, Noco R5). While cells expressing GFP were efficiently released into G1, more than half of the cells expressing GFP-E2 remained in mitosis. Expression of the transactivation domain of E2 alone (GFP-TAD), known to bind to Cdc20[16] and shown here to bind MAD2 and BUBR1 as well, also prevented HeLa cells from exiting mitosis. In contrast, the deletant lacking the TAD domain (GFP-ΔTAD) and therefore unable to bind Cdc20,[16] had no effect (**Fig. 3A**, Noco R5; also see **Fig. S2** for a control experiment where nocodazole was omitted). **Figure S3A** shows the levels of each protein at the different time-points. This experiment demonstrates that expression of E2 or TAD specifically in mitotic cells after activation of the SAC by nocodazole, inhibits exit from mitosis after release from the nocodazole block. This is a crucial experiment, which alongside our previous interaction data, leads to the conclusion that E2 can prevent SAC inactivation, most likely through its interaction with the MCC.

A similar experiment was also performed 24 hours after release from the nocodazole block instead of 5 hours (**Fig. S4**). Flow cytometry analyses still showed a mitotic arrest in the E2- and TAD-expressing populations. Moreover, E2 and TAD both enhanced aneuploidy by about 6 and 10% respectively at this time-point when compared to GFP (**Fig. S4**). Interestingly, in the absence of nocodazole, appearance of more than 2 daughter cells occurred quite frequently in cells escaping the TAD-induced mitotic block (**Movies S1 and S3**), potentially explaining the presence of this increased aneuploid population after nocodazole release in the E2 sample compared to the control.

TAD is more efficient than E2 at inducing a mitotic block in HeLa cells

In our previous studies involving HPV-negative cell pre-synchronized at the G1/S transition using thymidine, no obvious difference could be detected in the extent of mitotic arrest induced by full-length E2 compared to TAD after release from a thymidine block. Neither did we notice a significant difference in the number of abnormal anaphases between E2- and TAD-expressing cells.[16] In contrast, in HeLa cells, the mitotic block after release from nocodazole was reproductively more pronounced in cells expressing TAD than full-length E2 (62.9% and 54.4% respectively, **Fig. 3A**). In order to confirm that these differential effects of E2 and TAD on mitosis were not artifacts of the nocodazole block, release from S-phase instead of mitosis was performed. HeLa cells were synchronized in the middle of S phase by 2 successive 24 hour-thymidine blocks separated by a 2 hour-release. They were infected between the 2 blocks and harvested immediately after the second 24 hour-thymidine block (Thym R2), or released for 4 hours (Thym R6) or 12 hours (Thym R14) before flow cytometry analyses. Cells harvested immediately after the second thymidine block were arrested in the middle of S as expected (**Fig. 3B**, Thym R2). Four hours later, cells expressing the different proteins were all similarly released into G2 (**Fig. 3B**, Thym R6). By 12 hours of release (Thym R14), whereas a majority of GFP-expressing cells were back to G1, GFP-E2 had induced a mild mitotic arrest (53%) compared to TAD (75%). The western-blot in **Figure S3B** shows comparable levels of all proteins at the different time-points (although E2 increases from S to G2 as previously shown).[22] In conclusion and in contrast to HPV-negative cells lines, in HeLa cells TAD is more efficient than E2 at arresting cells in mitosis.

E6/E7 Expression and p53 inactivation potentiate E2 effects on mitosis

One important difference between E2- and TAD-expressing HeLa cells is the status of E6 and E7. Repression of E6/E7 transcription by E2 is mediated by its C-terminal DNA binding domain; thus E2 (and ΔTAD) represses E6/E7 transcription whereas TAD does not. Therefore, we tested the hypothesis that the difference of phenotype induced by GFP-E2 and GFP-TAD was linked to an effect of E6/E7 on the SAC proteins. First, the repression of E6/E7 by GFP-E2 (and GFP-ΔTAD) was confirmed by Real-Time PCR in the cells from **Figure 3B**. **Figure 4A** shows a marked repression of E6/E7 transcription in the presence of GFP-E2 or GFP-ΔTAD, but not GFP or GFP-TAD.

E7 has been shown to enhance BUBR1 transcription by about 2.6 times when compared to GFP in primary fibroblasts using microarray experiments,[23] and accordingly to this result, the levels of BUBR1 were shown to be high in human foreskin fibroblasts stably expressing E7.[24] Interestingly, in synchronized HeLa cells released from G1/S transition for 6 hours (therefore around 4–6 hours before mitotic entry), the levels of BUBR1 were lower in cells expressing GFP-E2 and GFP-ΔTAD (which both repress E7) than in GFP-TAD and GFP-expressing cells (**Fig. 4B**, Thym R6). The phenotype was even more severe in an asynchronous population where no BUBR1 could be detected by western-blot in GFP-E2 and GFP-ΔTAD expressing cells (**Fig. 4B**, Asynch). This lack of BUBR1 in the E2 samples compared to the TAD samples could partially impair MCC assembly and balance the effect of E2 on SAC up-regulation, explaining the intermediate phenotype observed with E2 compared to TAD.

E6 is known to mediate the degradation of p53 through the E6AP ubiquitin-ligase,[5] and in HeLa cells expressing GFP-E2 (but not in HeLa cells expressing GFP-TAD), E6 is repressed (**Fig. 4A**) while p53 is stabilized (**Fig. 4C**, compare lanes 1 and 3, 5 and 7, 9 and 11). We thus addressed the role of p53 in the mitotic phenotype. Silencing of p53 in HeLa cells expressing GFP-E2 efficiently inhibited the increase of p53 levels induced by E2 (**Fig. 4C**, compare lanes 1 and 2, 5 and 6, 9 and 10). Concomitantly, whereas no effect of the siRNA could be detected at early time-points of release from thymidine, the E2-expressing mitotic population was increased by about 13.5% 14 hours after release (**Fig. 4D**). As expected, the p53 siRNA had no effect on the TAD-expressing population (**Fig. S5**). This experiment shows that p53 can partially prevent the mitotic block induced by E2 and can therefore prevent SAC over-activation by E2. Involvement of p53 in the negative regulation of SAC activity could explain why we did not notice any significant difference between E2 and TAD phenotypes in HPV-negative cells, since we used p53-deficient cell lines.[16]

Down-regulation of SAC activity rescues the mitotic block, abnormal anaphases and mitotic cell death induced by HPV proteins

To definitely assess whether over-activation of the SAC was responsible for the mitotic arrest as well as for the abnormal mitoses and DNA damage observed, we reduced the SAC activity by silencing BUBR1 and looked whether this could revert the phenotypes in HeLa cells using time-lapse experiments. AdGFP-TAD-infected cells and AdGFP-infected control cells were transfected with siCtrl or siBUBR1 and synchronized in S-phase. After release, time-lapse microscopy showed that cells expressing GFP-TAD and transfected with the siCtrl entered metaphase (characterized by nice rounding-up cells). But instead of timely exiting mitosis, these cells experienced a massive block in metaphase followed by mitotic cell death, mitotic slippage or abnormal anaphase leading to 3 or more daughter cells (**Fig. 5A-B**, GFP-TAD siCtrl panels, and **Movies S1 and S3**). Under the same conditions, the GFP-expressing cells exhibited few abnormal mitoses and almost no cell death (**Fig. 5A**, GFP siCtrl panels, and **Movie S2**). Strikingly, when BUBR1 was silenced, abnormal phenotypes including metaphase block and cell death, but also abnormal anaphases, were completely rescued (**Fig. 5A-B**, compare GFP-TAD siCtrl with GFP-TAD siBUBR1 panels, also compare **Movie S1** with **Movie S4** and **Movie S3** with **Movie S6**). To monitor the behavior of mitotic DNA in these mitoses, low concentration of Hoechst was used to visualize the chromosomes during the time-lapse. **Figure 5B** (GFP-TAD siCtrl panels) and MOVIE

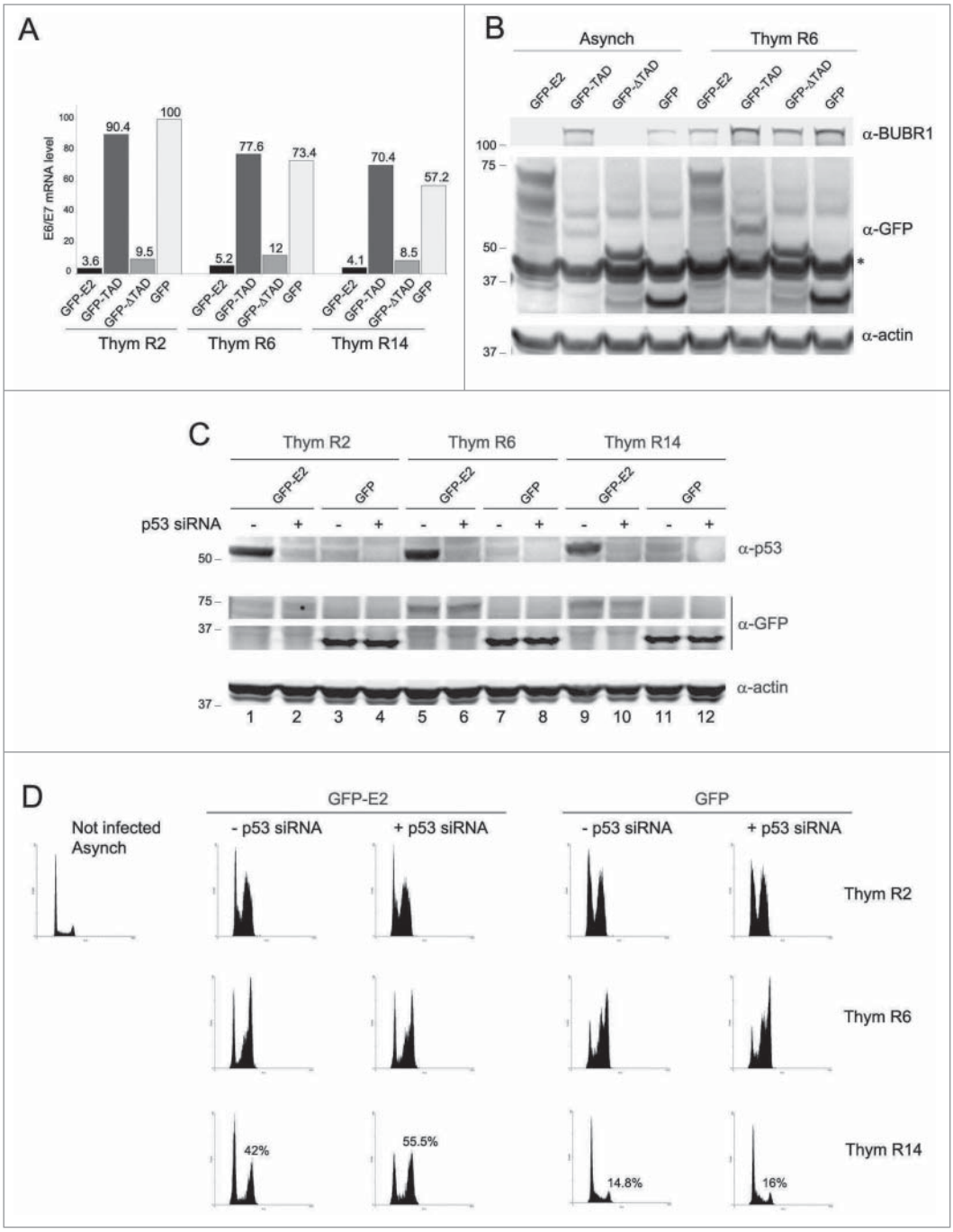

Figure 4. E6/E7 expression and p53 inactivation potentiate E2 effects on mitosis (**A**) RNAs were extracted from cells used in **Figure 3B**, reverse transcribed and the resulting cDNAs were subjected to Real-Time PCR to detect the endogenous level of E6/E7 mRNA. (**B**) Western-blots were performed with extracts from cells expressing the indicated proteins. Asynch = Asynchronous cells, Thym R6 = cells released for 4 hours following thymidine treatment. The asterisk corresponds to the actin for which the membrane was probed first. (**C**) Western-blot showing the relative quantities of the indicated proteins at the different time-points and in the different siRNA conditions. (**D**) Cell cycle analyses of HeLa cells expressing GFP-E2 or GFP, transfected with either a GADPH siRNA (-) or a siRNA against p53 (+), synchronized in S phase (Thym R2), and released for 4 (Thym R6) or 12 (Thym R14) hours. Infection and tranfection were performed during the thymidine block.

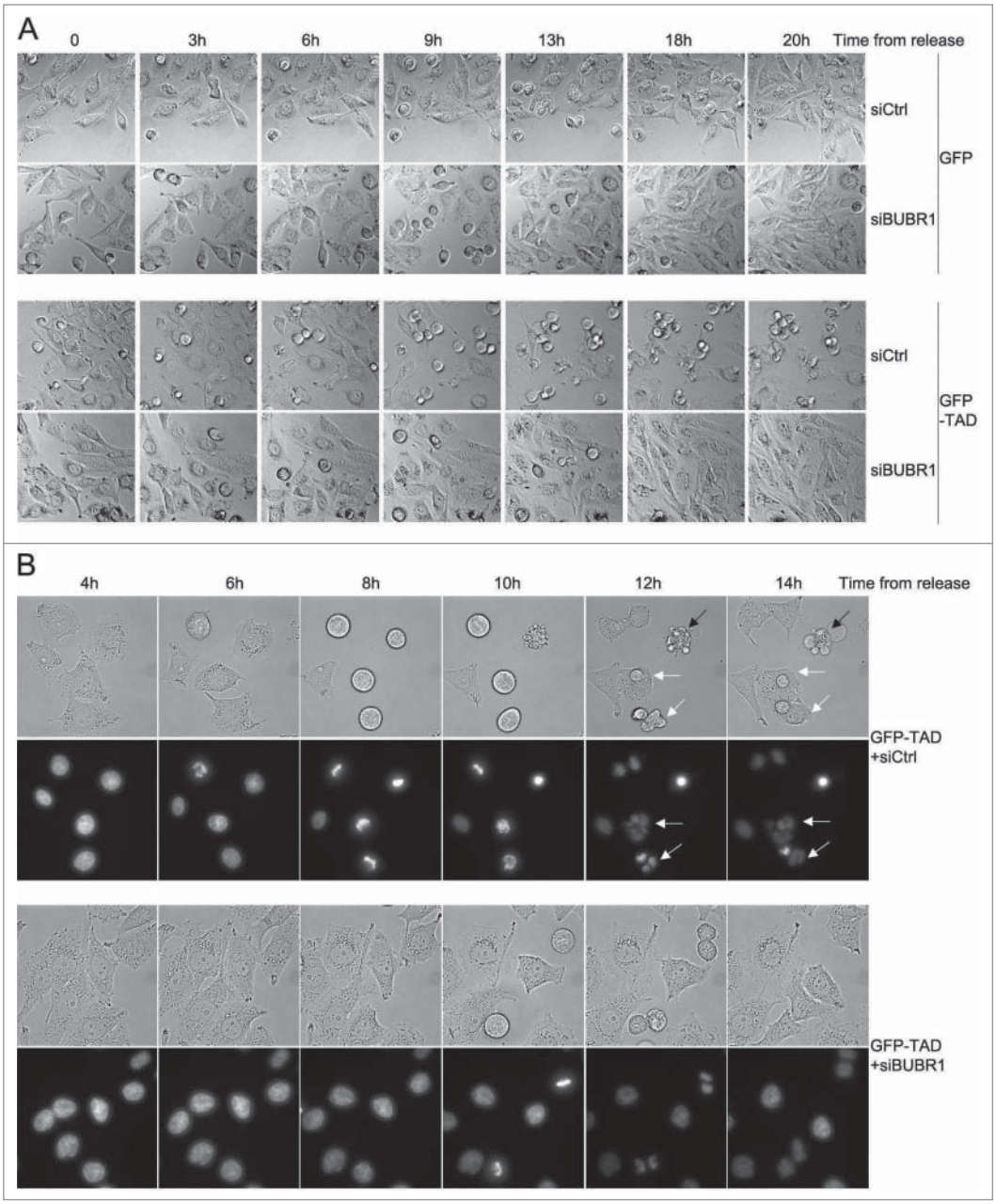

Figure 5. Silencing of BUBR1 rescues abnormal mitoses as well as mitotic cell death induced by E2. (**A**) Phase contrast images from time-lapse experiments. HeLa cells expressing GFP-TAD or GFP were transfected with a control siRNA (siCtrl) or a siRNA against BUBR1 (siBUBR1), synchronized by thymidine and released as indicated. (**B**) Time-lapse experiments performed with cells treated as in (A), but stained using Hoechst 33342. Upper panels show phase contrast pictures, lower panels show the corresponding DNA staining. Black arrows: mitotic cell death, white arrows: abnormal mitoses.

S3 show that TAD did not prevent condensation of DNA or metaphasic plate formation since the cells were able to reach metaphase and correctly aligned chromosomes. However, as expected from the phase contrast images, anaphase was compromised; TAD induced either cell death in metaphase (**Fig. 5B** black arrow, and **Movie S3**), or bending of chromosomes followed by abnormal segregation (**Fig. 5B** white arrows, and **Movie S3**). Again remarkably, when BUBR1 was silenced, these abnormal phenotypes were rescued (**Fig. 5B**, GFP-TAD siBUBR1 panels, also compare **Movie S3** to **Movie S6**). A western-blot confirming silencing of BUBR1 and expression of GFP-TAD and GFP is shown in **Figure S3C**.

We performed statistical analyses from these time-lapse experiments to better appreciate the effects of BUBR1 silencing. The graph from **Figure 6A** shows the kinetics of mitotic entry and exit of GFP-TAD and GFP cells treated with the BUBR1 or control siRNA, as well as the number of cells dying in metaphase in each condition. All percentages represent ratios between the number of mitoses observed at each time point and the total number of mitoses observed during the 24 hours of time-lapse (~300 mitoses). A peak of mitoses in GFP-expressing cells occurred around 10–12 hours after thymidine release as expected (dark pink graph). TAD-expressing cells reached a peak of mitoses with a similar timing, but most of them did not exit mitosis as shown in **Figure 5**, leading to accumulation of mitotic cells (plateau, solid dark blue line). About half of them died in metaphase soon or later following mitosis entry (dashed dark blue line). When BUBR1 was silenced in GFP-TAD-expressing cells, the plateau was lost and instead a diffuse left-shifted peak (compared to the GFP siCtrl peak) of mitoses appeared between 4 and 13 hours after release (solid light blue line), confirming a mitotic exit. Concomitantly, the mitotic cell death was completely rescued (dashed light blue line). **Figure 6B** shows that mitotic cell death (shown as a percentage of total mitotic cells) was reduced from 47% to 3%, and very importantly abnormal mitoses were decreased from 57% to 19%. SAC inhibition by the BUBR1 siRNA in TAD-expressing cells also reduced the average duration of mitosis by about 75% (from 249 to 67 minutes). As expected, since the negative regulation of metaphase-anaphase transition by the SAC is weakened in the presence of the BUBR1 siRNA, the peak

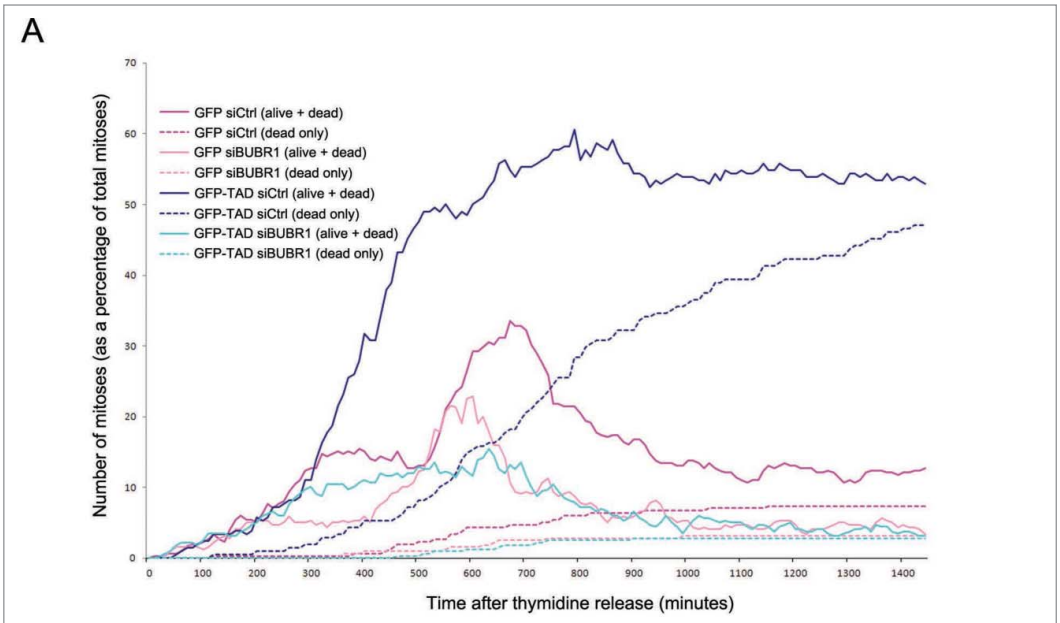

B

	GFP siCtrl	GFP siBUBR1	GFP-TAD siCtrl	GFP-TAD siBUBR1
Complete mitoses	92% → 77% Normal / 23% Abnormal	97% → 78% Normal / 22% Abnormal	53% → **43% Normal** / **57% Abnormal**	97% → **81% Normal** / **19% Abnormal**
Metaphasic cell death	8%	3%	**47%**	**3%**
Duration of mitosis	136 min	62 min	**249 min**	**67 min**

Figure 6. Statistical analyses of time-lapse experiments. (**A**) Kinetics of mitotic entry and exit of GFP-TAD- and GFP-expressing HeLa cells treated with the BUBR1 siRNA or Ctrl siRNA. The figure shows both the proportion of mitoses (alive + dead, solid line graphs) and the proportion of dead mitoses only (dashed line graphs) at each indicated time-point as a percentage of the total number of mitoses observed during the 24 hours time-lapse (~300 mitotic cells). (**B**) Characteristics of the mitoses from (A). Complete mitoses = cells which exit mitosis either normally or abnormally. Normal = 2 daughter cells, Abnormal = more than 2 daughter cells or mitotic slippage. Metaphasic cell death = cells dying in metaphase. Duration of mitosis = time from rounding up of the cells to separation into daughter cells. The proportions shown are percentages of the total number of mitotic cells (~300), except for normal and abnormal values which are percentages of complete mitoses. See also Movies S1 to S6.

of GFP siBUBR1-expressing mitoses was slightly shifted left and the duration of mitosis was also decreased by about half compared to Ctrl siRNA cells (136 to 62 minutes). Overall, although not exactly identical, the behavior of the TAD-expressing cells silenced for BUBR1 became similar to the control cells expressing GFP. It is important to note that inhibition of BUBR1 has previously been shown to induce chromosome misalignment and lethality,[25,26] and therefore it was surprising to obtain a majority of normal mitoses after BUBR1 silencing in TAD and GFP-expressing HeLa cells. However, the silencing of BUBR1 obtained here was only partial as shown in **Figure S3C**, probably because the endogenous levels of BUBR1 are high in HeLa cells due to E7 expression. In conclusion, these experiments revealed that after partial silencing of BUBR1, and so partial inhibition of the SAC, TAD no longer induces aberrant mitotic phenotypes. In conclusion, it appears that the mitotic block observed after E2 expression, the mitotic cell death, as well as the mis-segregation of DNA in anaphase are all consequences of SAC over-activation.

Discussion

This study, featuring HPV proteins, reveals that the mitotic Spindle Assembly Checkpoint (SAC) can be over-activated by pathogens to promote abnormal mitoses. We show that HPV-18 E2 binds Cdc20 and the Mitotic Checkpoint Complex (MCC) proteins BUBR1 and MAD2, and that these interactions correlate with mitotic block, DNA breaks and aneuploidy. E2-expressing cells fail to recover from a nocodazole block, signifying that E2 can prevent inactivation of the SAC if activated by independent stimuli like microtubule-targeting drugs. Altogether, these data lead to the idea that E2 interaction with MCC proteins could allow formation of a MAD2/BUBR1/Cdc20/E2 complex which prevents SAC inactivation. These data are of particular interest to the HPV field since they demonstrate an obvious oncogenic property of E2 which could account for the transforming capacity of HPV. Unexpectedly, we also demonstrate that, at least in HeLa cells, SAC over-activation is potentiated by loss of p53 (a recurrent event in cancer). Therefore, not only do our data suggest that SAC activity could be regulated by p53 (which is beyond the scope of this paper but opens new fields of investigation), but they also pinpoint SAC over-activation in a p53-negative context as a highly pathogenic event.

Regarding the role played by E7 in the E2-associated mitotic phenotype, E7 has previously been shown to induce metaphase defects,[27] although anaphase appeared normal. It has been recently demonstrated that E7 engages both SAC-independent[28] and SAC-dependent[24] mechanisms to prevent APC/C-dependent degradation of cyclin A and cyclin B. In the latter article,

both MAD2 and BUBR1 were found highly expressed in E7-positive cells. Our results are in agreement with these data since we demonstrate that HeLa cells expressing TAD or GFP (thus free from E2-mediated E7 repression) contain higher levels of BUBR1 than HeLa cells expressing E2 or ΔTAD (where E7 is repressed). However, an increase in BUBR1 levels is not sufficient to induce the mitotic phenotype observed with TAD in HeLa cells since GFP-expressing HeLa cells (and not infected cells) do not show such defects in mitosis. Therefore, it appears that the interaction of E2 with the MCC could be primordial to induce this mitotic phenotype. Whether the effects of E7 on metaphase[27] are mediated through BUBR1 increase is still unclear, but it seems that this increase of BUBR1, combined with over-activation of the SAC by E2, leads to the severe metaphase and anaphase defects observed here in HPV-positive cells.

MAD2 over-expression has been formally demonstrated to induce tumors in mice through SAC over-activation, leading to DNA mis-segregation and breaks reminiscent of E2-induced phenotypes.[29,30] In contrast, recent data showed that overexpression of BUBR1 protects against aneuploidy.[31] To date, the reason why over-expression of BUBR1 and MAD2 in the context of these 3 studies have opposite effects is unclear. In our study, it appears that the effects of E2 on the SAC mimic MAD2 overexpression, but also that BUBR1 plays a central role in this phenotype. Considering E2 interaction with Cdc20, but also with both MAD2 and BUBR1, the DNA breaks and mis-segregation observed are likely to be mediated through E2 interaction with the MCC.

Lastly, since integration of HPV DNA into the viral genome occurs through cellular DNA breaks, we propose a model whereby SAC over-activation by E2 could favor integration of viral DNA leading to malignant progression of HPV-positive lesions. E2 could therefore initiate cervical carcinogenesis. More work is needed to verify whether E2 can indeed increase integration and further confirm this hypothesis. However, this model is supported by the observation that E2 proteins from low-risk HPV-11 and 6, whose DNA never integrates, do not induce such abnormal mitotic phenotypes.[16]

Our results have substantial implications since they provide, for the first time, a hypothesis about the underlying mechanism of HPV genome integration, which unexpectedly could involve E2. Interestingly, E2 could also exert an intrinsic oncogenic activity through induction of chromosomal abnormalities. This novel framework of understanding opens several new areas of investigation for both fundamental and therapeutic HPV research to target E2 (and/or integration) for prevention of cervical carcinoma.

Materials and Methods

Cell culture, synchronization, infection and transfection

All cell lines used here were authenticated using short-tandem repeat (STR) profiling within the last 6 months.

Cell lines were grown in Dulbecco's Modified Eagle's Medium (DMEM) supplemented with 10% fetal calf serum (FCS).

C33-A cells were synchronized at the G1/S transition phase by incubation with thymidine (2.5 mM, Sigma-Aldrich) for 24 hours. After release and 0, 6 or 14 hours of culture in thymidine-free medium, cells were harvested and flow cytometry was performed.

For release from nocodazole block, HeLa cells were first synchronized at the G1/S transition using thymidine, and then released for 6 hours before nocodazole treatment (60 ng/ml) and infection. This protocol allows the transduced proteins to accumulate only after the cells are stalled in pro-metaphase by nocodazole, and not before mitosis (adenovirus-mediated protein expression starts from 8 hours after infection, whereas the cells enter mitosis around 6 hours after infection). Fourteen hours later, mitotic cells were collected by shake-off and incubated in fresh nocodazole-free medium for 5 hours before flow cytometry and western-blotting.

For HeLa cells, in which re-expression of E2 inhibits E6 transcription, leads to p53 stabilization and prevents cells from being released after a G1/S block induced by thymidine, we had to arrest cells expressing the different constructs in the middle of the S phase instead of at the G1/S transition to be able to efficiently release them from the thymidine block. Cells were synchronized in mid-S phase by a 24-hour thymidine treatment, followed by a 2 hour release, and a second 24-hour thymidine treatment. Infections were performed just before the second thymidine block. Cells were released for 4 or 12 hours after the second block (thus 6 and 14 hours after the first block) and analyzed by flow cytometry.

Adenovirus infections were performed for 1 hour in serum-free medium (m.o.i. 20 to 200 depending on experiments). Polybrene (40 μg/mL) was added for infection of U2OS and C33-A cells.

Transfections with siRNA were performed using DharmaFECT1 (Dharmacon). siRNA used: BUBR1 siRNA (L-004101–00–0010, Dharmacon), p53 siRNA (L-003329–00–0020, Dharmacon) or GADPH siRNA (D-001830–01–20, Dharmacon). Transfections with plasmids were performed using Fugene HD (Promega). The HA-Cdc20 plasmid was a gift from Marito Araki.

Immunoprecipitation and western-blotting

For immunoprecipitation, C33-A cells were infected at m.o.i 20, followed by transfection with HA-Cdc20 (whereas BUBR1 and MAD2 were endogenous proteins). Cells were then treated with thymidine for 24 hours and released in DMEM containing nocodazole (60 ng/ml) for 16 hours before extraction. 300μg of total proteins were immunoprecipitated using GFP-Trap®_A beads (ChromoTek). Total immunoprecipitates or equal amounts of proteins (for inputs) were separated by SDS-PAGE before transfer onto membranes for western-blotting. Blots were revealed using ECL Plus (Amersham Biosciences).

Primary antibodies used for western-blot: anti-GFP (TP401; Torrey Pines Biolabs), anti-β-tubulin (T4026; Sigma-Aldrich), anti-actin (A2066; Sigma-Aldrich), anti-Cdc20 (ab64877, Abcam), anti-BUBR1 (612502, BD Transduction Laboratories),

anti-MAD2 (ab70385, Abcam) and anti-p53 (DO-1: sc-126, Santa Cruz).

Immunofluorescence

U2OS cells were cultured on poly-L-lysine coated glass slides, and infected on slides by recombinant adenoviruses (m.o.i. 20). After 24 hours, cells were swollen in hypotonic buffer (10 mM Tris-HCL pH7.4, 10 mM NaCl and 5 mM $MgCl_2$)[32] for 10 minutes at room temperature. Slides were then centrifuged for 5 minutes at 1000 rpm and fixed using 4% PFA for 10 minutes. Cells were permeabilized using 0.1% Triton in PBS, blocked with PBS/5% FCS and incubated with anti-BUBR1 (gift from Stephen Taylor),[33] anti-CENP-E (ab5093, Abcam), anti-MAD2 (ab70385, Abcam) or anti-β-tubulin (T4026; Sigma-Aldrich). DNA was stained with DAPI. Pictures were taken with the Applied Precision DeltaVision Deconvolution microscope system and images were analyzed using SoftWoRx v4.0.0.

Time-lapse microscopy

Infected HeLa cells were synchronized in S as described above, and released. Time-lapse microscopy was performed using Applied Precision DeltaVision Deconvolution microscope system set at 37°C and 5% CO_2. DNA was stained with Hoechst 33342 (0.2 μg/ml). Images were acquired every 10 minutes for 24 hours. For each infection, ~400 cells (~300 entered mitosis during the time-lapse) were examined from 5 different fields. Images were analyzed using Fiji.

Flow-cytometry

Cells were fixed in PBS/70% Ethanol, washed, treated with RNAse A (10 μg/ml) and stained with DAPI (5 μg/ml) or propidium iodide (10 μg/ml). For detection of mitotic cells, fixed cells were incubated with anti-histone H3 phospho S10 (ab5176, Abcam) for 1 hour, washed and incubated with anti-rabbit-Alexa 647 (A21244, Invitrogen) for 1 hour prior to DAPI staining. Flow cytometry was performed using a BD LSRII (BD Biosciences), data were analyzed with BD FACSDiva and WinMDI software.

Real-time PCR

RNAs from HeLa cells were extracted using RNeasy mini kit (Qiagen) and treated with Dnase I. Two and a half μg of total RNA were reverse-transcribed using Superscript II (Invitrogen). Real-Time PCR was carried out as previously described.[34] Amplification values were normalized to GADPH cDNA. Primers used: E7/E6 (5′ CCCCAAAATGAAATTCCGGT 3′, 5′ GTCGCTTAATT GCTCGTGACATA 3′), GADPH (5′ TCCCATCACCATCTTCCAGG 3′, 5′ CATCGCCCCACTTGATTTTG 3′).

Comet assay

Cells expressing GFP-E2, GFP-ΔTAD or GFP were synchronized at the G1/S transition using thymidine and released for 14 hours. Comet assays were done using the OxiselectTM Comet Assay Kit (Cell Biolabs, Inc., Cat No. STA-350), according to manufacturer's instructions. Cells treated with 100 mM hydrogen peroxide (H_2O_2) for 10 minutes on ice were used as a positive control. Electrophoresis was done using BioRad Sub-Cell 192 at 25V for 15 minutes in 3L 1X TBE buffer. Photos were taken using 4X lens on NIKON Eclipse TS100 microscope.

Disclosure of Potential Conflicts of Interest

No potential conflicts of interest were disclosed.

Acknowledgments

The authors thank Francoise Thierry for critical reading and helpful suggestions, Walter Blackstock and Kelly Hogue for technical assistance in mass spectrometry analysis, and Lucy Robinson from Insight Editing London for writing assistance.

Supplemental Material

Supplemental data for this article can be accessed on the publisher's website.

Author Contributions

CLT, ST and SB conceptualized the experiments. CLT designed and generated new protein constructs, performed the Comet assays, developed the immunoprecipitation and mass spectrometry experiments. JG analyzed the mass spectrometry data. CLT and SB performed the immunofluorescence experiments. SB and ST conceptualized and performed the synchronization experiments, and analyzed the flow cytometry data. CLT, ST, LSQ and SB performed infections, transfections and western-blots. SB wrote the manuscript and Supplementary information.

References

1. zur Hausen H. Condylomata acuminata and human genital cancer. Cancer Res 1976; 36: 794; PMID:175942
2. Schiffman M, Castle PE, Jeronimo J, Rodriguez AC, Wacholder S. Human papillomavirus and cervical cancer. Lancet 2007; 370: 890-907; PMID:17826171; http://dx.doi.org/10.1016/S0140-6736(07)61416-0
3. Scheffner M, Werness BA, Huibregtse JM, Levine AJ, Howley PM. The E6 oncoprotein encoded by human papillomavirus types 16 and 18 promotes the degradation of p53. Cell 1990; 63: 1129-36; PMID:2175676; http://dx.doi.org/10.1016/0092-8674(90)90409-8
4. Werness BA, Levine AJ, Howley PM. Association of human papillomavirus types 16 and 18 E6 proteins with p53. Science 1990; 248: 76-9; PMID:2157286; http://dx.doi.org/10.1126/science.2157286
5. Scheffner M, Huibregtse JM, Vierstra RD, Howley PM. The HPV16 E6 and E6-AP complex functions as ubiquitin-protein ligase in the ubiquitination of p53. Cell 1993; 75: 495-505; PMID:8221889; http://dx.doi.org/10.1016/0092-8674(93)90384-3
6. Münger K, Werness BA, Dyson N, Phelps WC, Harlow E, Howley PM. Complex formation of human papillomavirus E7 proteins with the retinoblastoma tumor suppressor gene product. EMBO J 1989; 8: 4099-105; PMID:2556261
7. Dyson N, Howley PM, Münger K, Harlow E. The human papillomavirus-16 E7 oncoprotein is able to bind to the retinoblastoma gene product. Science 1989; 243: 934-7; PMID:2537532; http://dx.doi.org/10.1126/science.2537532
8. Thierry F, Yaniv M. The BPV1-E2 trans-acting protein can be either an activator or a repressor of the HPV18 regulatory region. EMBO J 1987; 6: 3391-7; PMID:2828029
9. Desaintes C, Demeret C, Goyat S, Yaniv M, Thierry F. Expression of the papillomavirus E2 protein in HeLa cells leads to apoptosis. EMBO J 1997; 16: 504-14; PMID:9034333; http://dx.doi.org/10.1093/emboj/16.3.504

10. Cullen AP, Reid R, Campion M, Lorincz AT. Analysis of the physical state of different human papillomavirus DNAs in intraepithelial and invasive cervical neoplasm. J Virol 1991; 65: 606-12; PMID:1846186
11. Vinokurova S, Wentzensen N, Kraus I, Klaes R, Driesch C, Melsheimer P, Kisseljov F, Durst M, Schneider A, von Knebel Doeberitz M. Type-dependent integration frequency of human papillomavirus genomes in cervical lesions. Cancer Res 2008; 68: 307-13; PMID:18172324; http://dx.doi.org/10.1158/0008-5472.CAN-07-2754
12. Corden SA, Sant-Cassia LJ, Easton AJ, Morris AG. The integration of HPV-18 DNA in cervical carcinoma. Mol Pathol 1999; 52: 275-82; PMID:10748877; http://dx.doi.org/10.1136/mp.52.5.275
13. McLaughlin-Drubin M, Munger K. The human papillomavirus type 8 E2 gene encodes a transforming activity sufficient for skin tumor formation in transgenic mice. J Invest Dermatol 2008; 128: 2142-4; PMID:18695686; http://dx.doi.org/10.1038/jid.2008.217
14. Pfefferle R, Marcuzzi GP, Akgul B, Kasper HU, Schulze F, Haase I, Wickenhauser C, Pfister H. The human papillomavirus type 8 E2 protein induces skin tumors in transgenic mice. J Invest Dermatol 2008; 128: 2310-5; PMID:18401427; http://dx.doi.org/10.1038/jid.2008.73
15. Leykauf K, Kabsch K, Gassler N, Gissmann L, Alonso A, Schenkel J. Expression of the HPV11 E2 gene in transgenic mice does not result in alterations of the phenotypic pattern. Transgenic Res 2008; 17: 1-8; PMID:17701441; http://dx.doi.org/10.1007/s11248-007-9130-y
16. Bellanger S, Blachon S, Mechali F, Bonne-Andrea C, Thierry F. High-risk but not low-risk HPV E2 proteins bind to the APC activators Cdh1 and Cdc20 and cause genomic instability. Cell Cycle 2005; 4: 1608-15; PMID:16222116; http://dx.doi.org/10.4161/cc.4.11.2123
17. Musacchio A, Salmon ED. The spindle-assembly checkpoint in space and time. Nat Rev Mol Cell Biol 2007; 8: 379-93; PMID:17426725; http://dx.doi.org/10.1038/nrm2163
18. Bellanger S, Tan CL, Xue YZ, Teissier S, Thierry F. Tumor suppressor or oncogene? a critical role of the viral E2 protein in cervical cancer progression. Am J Cancer Res 2011; 1: 373-89; PMID:21968515
19. Xue Y, Bellanger S, Zhang W, Lim D, Low J, Lunny D, Thierry F. HPV16 E2 is an immediate early marker of viral infection, preceding E7 expression in precursor structures of cervical carcinoma. Cancer Res 2010; 70: 5316-25; PMID:20530671; http://dx.doi.org/10.1158/0008-5472.CAN-09-3789
20. Oliveira JG, Colf LA, McBride AA. Variations in the association of papillomavirus E2 proteins with mitotic chromosomes. Proc Natl Acad Sci U S A 2006; 103: 1047-52; PMID:16415162; http://dx.doi.org/10.1073/pnas.0507624103
21. Muller M, Jacob Y, Jones L, Weiss A, Brino L, Chantier T, Lotteau V, Favre M, Demeret C. Large scale genotype comparison of human papillomavirus E2-host interaction networks provides new insights for e2 molecular functions. PLoS Pathog 2012; 8: e1002761; PMID:22761572; http://dx.doi.org/10.1371/journal.ppat.1002761
22. Bellanger S, Tan CL, Nei W, He PP, Thierry F. The human papillomavirus type 18 E2 protein is a cell cycle-dependent target of the SCFSkp2 ubiquitin ligase. J Virol 2010; 84: 437-44; PMID:19828607; http://dx.doi.org/10.1128/JVI.01162-09
23. Pang CL, Toh SY, He P, Teissier S, Ben Khalifa Y, Xue Y, Thierry F. A functional interaction of E7 with B-Myb-MuvB complex promotes acute cooperative transcriptional activation of both S- and M-phase genes. (129 c). Oncogene 2014; 33: 4039-49; PMID:24141769; http://dx.doi.org/10.1038/onc.2013.426
24. Yu Y, Munger K. Human papillomavirus type 16 E7 oncoprotein engages but does not abrogate the mitotic spindle assembly checkpoint. Virology 2012; 432: 120-6; PMID:22748180; http://dx.doi.org/10.1016/j.virol.2012.06.006
25. Kops GJ, Foltz DR, Cleveland DW. Lethality to human cancer cells through massive chromosome loss by inhibition of the mitotic checkpoint. Proc Natl Acad Sci U S A 2004; 101: 8699-704; PMID:15159543; http://dx.doi.org/10.1073/pnas.0401142101
26. Lampson MA, Kapoor TM. The human mitotic checkpoint protein BubR1 regulates chromosome-spindle attachments. Nat Cell Biol 2005; 7: 93-8; PMID:15592459; http://dx.doi.org/10.1038/ncb1208
27. Nguyen CL, Munger K. Human papillomavirus E7 protein deregulates mitosis via an association with nuclear mitotic apparatus protein 1. J Virol 2009; 83: 1700-7; PMID:19052088; http://dx.doi.org/10.1128/JVI.01971-08
28. Yu Y, Munger K. Human papillomavirus type 16 E7 oncoprotein inhibits the anaphase promoting complex/cyclosome activity by dysregulating EMI1 expression in mitosis. Virology 2013; 446: 251-9; PMID:24074588; http://dx.doi.org/10.1016/j.virol.2013.08.013
29. Schvartzman JM, Duijf PH, Sotillo R, Coker C, Benezra R. Mad2 is a critical mediator of the chromosome instability observed upon Rb and p53 pathway inhibition. Cancer Cell 2011; 19: 701-14; PMID:21665145; http://dx.doi.org/10.1016/j.ccr.2011.04.017
30. Sotillo R, Hernando E, Diaz-Rodriguez E, Teruya-Feldstein J, Cordon-Cardo C, Lowe SW, Benezra R. Mad2 overexpression promotes aneuploidy and tumorigenesis in mice. Cancer Cell 2007; 11: 9-23; PMID:17189715; http://dx.doi.org/10.1016/j.ccr.2006.10.019
31. Baker DJ, Dawlaty MM, Wijshake T, Jeganathan KB, Malureanu L, van Ree JH, Crespo-Diaz R, Reyes S, Seaburg L, Shapiro V, et al. Increased expression of BubR1 protects against aneuploidy and cancer and extends healthy lifespan. Nat Cell Biol 2013; 15: 96-102; PMID:23242215; http://dx.doi.org/10.1038/ncb2643
32. Poddar A, Reed SC, McPhillips MG, Spindler JE, McBride AA. The human papillomavirus type 8 E2 tethering protein targets the ribosomal DNA loci of host mitotic chromosomes. J Virol 2009; 83: 640-50; PMID:19004936; http://dx.doi.org/10.1128/JVI.01936-08
33. Taylor SS, Hussein D, Wang Y, Elderkin S, Morrow CJ. Kinetochore localisation and phosphorylation of the mitotic checkpoint components Bub1 and BubR1 are differentially regulated by spindle events in human cells. J Cell Sci 2001; 114: 4385-95; PMID:11792804
34. Thierry F, Benotmane MA, Demeret C, Mori M, Teissier S, Desaintes C. A genomic approach reveals a novel mitotic pathway in papillomavirus carcinogenesis. Cancer Res 2004; 64: 895-903; PMID:14871818; http://dx.doi.org/10.1158/0008-5472.CAN-03-2349